The Calculation of Fuel Bowing Reactivity Coefficients in a Subcritical Advanced Burner Reactor

A Thesis
Presented to
The Academic Faculty

by

Andrew T. Bopp

In Partial Fulfillment
of the Requirements for the Degree
Master of Science in Nuclear Engineering

Georgia Institute of Technology
December 2013

The Calculation of Fuel Bowing Reactivity Coefficients in a

Subcritical Advanced Burner Reactor

Approved by:

Dr. Weston M. Stacey, Advisor
Nuclear and Radiological Engineering
Georgia Institute of Technology

Dr. Bojan Petrovic
Nuclear and Radiological Engineering
Georgia Institute of Technology

Dr. S. Mostafa Ghiaasiaan
Mechanical Engineering
Georgia Institute of Technology

Dr. Jim Grudzinski
Nuclear Engineering Division
Argonne National Laboratory

Date Approved: 12 September 2013

Acknowledgements

The present work began largely with the assistance of Dr. Jim Grudzinski whose previous work with fuel bowing calculations gave clarity to the subject and helped choose the tools to be used in the calculations. Thanks is also due to Dr. Bojan Petrovic and Dr. Glenn Sjoden for their frequent assistance in understanding perturbation theory. I thank Dr. Mostafa Ghiaasiaan for the numerous RELAP discussions. I am also thankful to my advisor Dr. Stacey for his extreme patience and unyielding enthusiasm for this work. Finally, I would like to thank my family and my girlfriend Steph for their constant support and encouragement.

Table of Contents

Page

List of Figures

List of Tables

Chapter I: Introduction

The United States' fleet of Light Water Reactors (LWRs) produces a large amount of spent fuel each year; all of which is presently intended to be stored in a fuel repository for disposal. As these LWRs continue to operate and more are built to match the increasing demand for electricity, the required capacity for these repositories grows. Georgia Tech's Subcritical Advanced Burner Reactor (SABR) **[1]** has been designed to reduce the capacity requirements for these repositories and thereby help close the back end of the nuclear fuel cycle by burning the long-lived transuranics in spent nuclear fuel. SABR's design is based heavily off of the Integral Fast Reactor (IFR).**[2]**

It is important to understand whether the SABR design retains the passive safety characteristics of the IFR. A full safety analysis of SABR's transient response to various possible accident scenarios needs to be performed to determine this. However, before this safety analysis can be performed, it is imperative to model all components of the reactivity feedback mechanism in SABR. The purpose of this work is to develop a calculational model for the fuel bowing reactivity coefficients that can be used in SABR's future safety analysis. This thesis discusses background on fuel bowing and other reactivity coefficients, the history of the IFR, the design of SABR, describes the method that was developed for calculating fuel bowing reactivity coefficients and its verification, and presents an example of a fuel bowing reactivity calculation for SABR.

Chapter II: Reactivity Feedbacks

Reactivity feedbacks play a major role in any accidental transient and hence are an essential component of reactor safety analyses. Reactivity feedbacks are caused by a diverse set of physical processes and have varying degrees of impact. Specific feedbacks of concern are sodium voiding, doppler broadening, thermal expansion, and fuel bowing. Sodium voiding is the most well known reactivity feedback for fast reactors. As the temperature of the sodium moderator changes, so does the density, and the change in density is what causes the change in reactivity.[3] The change in reactivity can be broken up into three components: spectral, capture, and leakage. The spectral component stems from a change in the elastic and inelastic cross sections, the capture component stems from the change in the macroscopic capture cross-section, and the leakage component stems from the change in the transport cross-section. The spectral and capture components tend to dominate in the center of the core while the leakage component dominates on the edge of the core. Sodium voiding can contribute positive reactivity if care is not taken when designing the geometry of the core. Designing a core with the lowest possible height-to-diameter ratio will maximize the leakage component enough to dominate the others and generate a negative feedback.[3]

Another well known feedback is Doppler broadening. Essentially, an increase in fuel temperature changes, or "broadens", the narrow shape of the fuel's resonance curve.[3] It is a combination of competing fission, capture, and leakage rates. For fast reactors, the Doppler effect is only relevant below energies of 25 keV because the cross-sections vary little at higher energies. At 25 keV, leakage is very low, so the leakage component can be ignored. Doppler broadening is almost always negative but becomes less negative and potentially positive in reactors with a hard neutron spectrum. This is because the fission-to-capture ratio increases with neutron energy. Increasing the probability of fission per neutron capture will not change the shape of the resonance curve, but it will

increase its magnitude leading to a positive contribution of reactivity that may be large enough to override the other negative components of Doppler broadening.

Thermal expansion is another important reactivity feedback, but it is an umbrella term that could refer to any number of feedbacks such as the axial and radial expansion of the fuel and reflector or even expansion in the control rods. Axial expansion of the fuel is one of them. As the fuel increases in temperature, its density decreases while its length increases. For the simple case of a bare, solid fuel pin, this feedback would be negative because some of the fuel has been moved axially outward away from the core into a region of lower neutron importance.[3] For more realistic designs with fuel pellets, cladding, and fuel assemblies, this feedback can become highly non-linear and must be calculated for a specific fuel design. Radial expansion in the fuel is somewhat different. The radially outward expansion of the fuel is too small to cause a change in reactivity, but if the fuel expels the bond sodium between itself and the cladding, the rate of heat transfers drops and the fuel temperature increases which in turn can trigger other feedbacks.[3] Thermal expansion also occurs in the control rods causing them to move closer toward the center of the core.[3] This is a negative feedback whose effect is proportional to the worth of the control rods. The simplest and most predictable feedback due to expansion is the thermal expansion of the core grid plate that supports all of the fuel assemblies.[3] An increase in grid plate temperature causes the entire core to expand radially outward. Negative reactivity is generated from the fuel moving into a region of lower neutron importance and an increase in neutron leakage due to increase in core surface area. Radial expansion of the core is a much more powerful feedback than axial expansion.[3] This is because any increase in core surface area increases neutron leakage and core surface area scales linearly with core height but with the square of core diameter. This is another reason that modern fast reactors are designed with the smallest possible height-to-diameter ratio. Reflector expansion should also be considered as a reactivity feedback. Any change in density in the reflector will alter its effectiveness. This is another design-specific feedback

3

because the reactivity change once again depends on the specific core design.

The most complex and design-specific reactivity feedback is fuel bowing. Fuel bowing occurs when one side of a fuel pin or fuel assembly is hotter than the other resulting in thermal strain.[**4**] This thermal strain causes the fuel to move into a region of higher or lower neutron importance and thus generates a change in reactivity. Modern fast reactor fuel assemblies have been designed to restrict any fuel bowing in the pins themselves, so non-uniform temperatures across the fuel assemblies are the main driver for fuel bowing.[**4**] In other words, fuel bowing is a function of the temperature change across the core. This is fundamentally different from all of the other feedbacks that depend simply on the absolute temperature of the core. This means that the behavior of fuel bowing feedbacks is highly design-specific and in certain cases be postive enough to dominate all other feedbacks in a fast reactor. [**3**]

Standard practice for calculating a reactivity feedback is to hold all other variables constant (ie neglect other reactivity feedbacks) and use first order, diffusion-based perturbation theory to estimate the resulting change in reactivity.[**5**] First order, diffusion-based perturbation theory is quick and measures well against more detailed, higher order calculations.[**5**]

Chapter III: History of Passive Safety of the Integral Fast Reactor

Reactivity feedback due to fuel bowing was first noticed in Argonne National Laboratory's (ANL) Experimental Breeder Reactor I (EBR-I). EBR-I was a liquid metal-cooled fast reactor that operated from 1951 to 1965 and performed a variety of impactful experiments [**6**]. It was the first nuclear reactor to produce electricity, the first reactor to produce a breeding gain (produce more fissile material than it consumed), and the first reactor to use high-temperature molten metal as a coolant.

One day in 1955, the EBR-I operators were studying changes in the power level caused by changes in the coolant flow rate. This inadvertently resulted in a partial meltdown of EBR-I due to a positive fuel bowing reactivity feedback. Subsequent analysis indicated that the reduction in coolant flow developed a temperature change across the core that caused the fuel to bow inward toward a region of higher neutron flux and importance.

Based on this experience, EBR-II was constructed in 1965 to have a negative fuel bowing coefficient and was eventually used to prove that a liquid metal fast reactor could achieve passive safety through the action of reactivity feedbacks in 1986. [**7**] Loss of Flow (LOFA) and Loss of Heat Sink (LOHSA) tests were conducted from full power without SCRAM. It was found for both cases that the ensuing negative reactivity produced a reactor shutdown, and the residual decay heat could be removed via natural circulation. Results from two LOFA tests with different pump-stop times are shown in Fig. 1 and Fig 2. The figures show a drop in reactivity as the power-to-flow ratio increases for each case. While it is obvious that the reactivity begins to drop as soon as the flow begins to coast down, it is not apparent how much of that is due strictly to fuel bowing. The instrumentation used during the tests measured the power level using an ion chamber and calculated the total reactivity using inverse point kinetics; reactivity values for individual feedbacks were not calculated. Developing a model that can calculate the reactivity feedback due only to fuel bowing will help to determine fuel

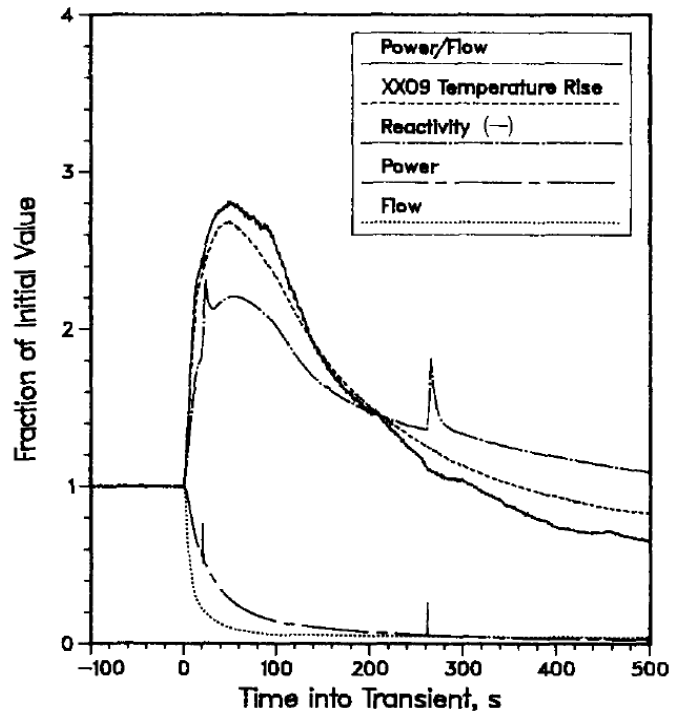bowing's importance relative to other reactivity feedbacks.

Fig. 1: EBR-II Loss-of-Flow-Accident, Test 45, 100 second pump stop time (Taken from *Nuc. Eng and Des, Vol 101, pp 75-90, 1987*)
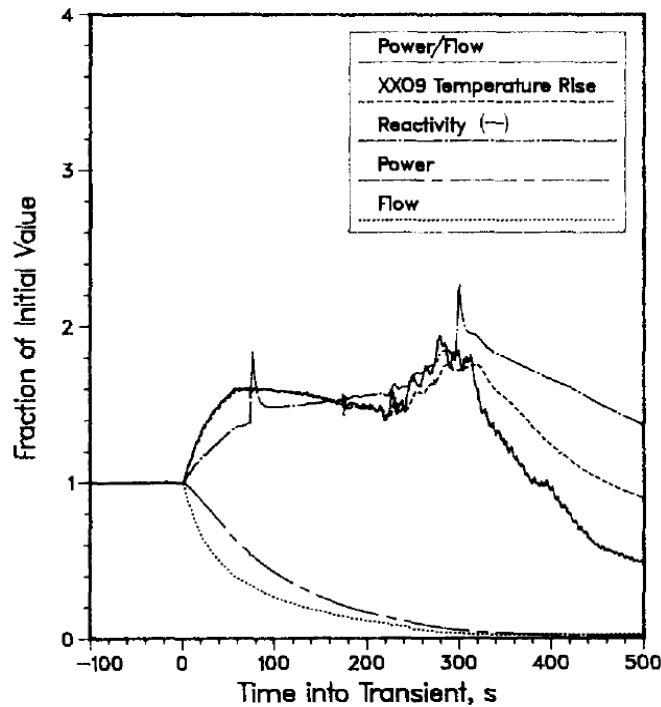
Fig. 2: EBR-II Loss-of-Flow-Accident, Test 39, 300 second pump stop time (Taken from *Nuc. Eng and Des, Vol 101, pp 75-90, 1987*)

The experimentally-validated passive safety of EBR-II was included in ANL's Integral Fast Reactor (IFR). **[2]** Like EBR-II, IFR is a metal fueled, sodium cooled, pool-type fast reactor designed to be passively safe. The purpose of IFR was to take the passive safety features of EBR-II and integrate them into a commercially viable fast reactor design. Numerous fuel cycle studies were performed, and it was concluded that IFR would be proliferation resistant and function well as a breeder or a burner.[**8**]

One of the more interesting features of the IFR design is the core restraint system. A large metal ring extends around the periphery of the core and limits the radially outward motion of any fuel assemblies. The radially outward motion is limited to impacting on two contact points: the Above Core Load Pad (ACLP) and the Top Load Pad (TLP). Fig. 3 is a diagram of a fuel assembly that shows the location of the core region and the load pads that contact the restraint ring. The ACLP is located just above the active region of the fuel while TLP is located at the very top of the assembly as shown in Fig

7

3.

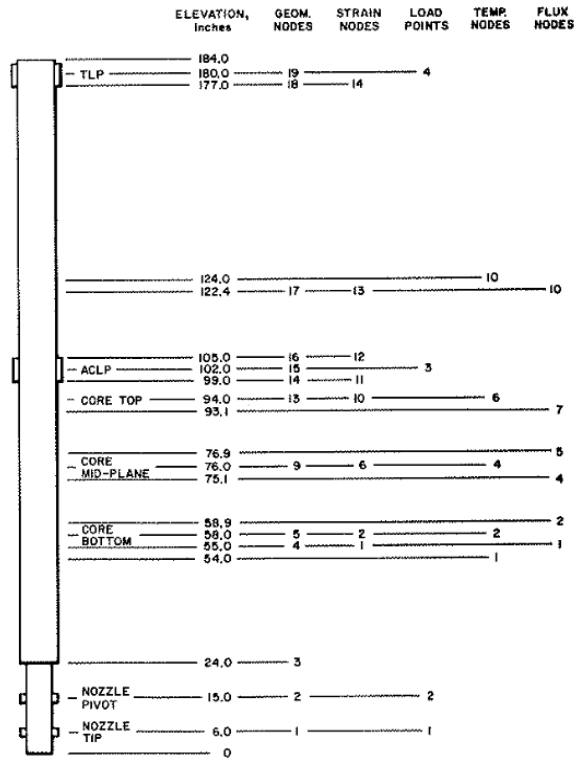|	ELEVATION, Inches	GEOM. NODES	STRAIN NODES	LOAD POINTS	TEMP. NODES	FLUX NODES
	184.0					
TLP	180.0	19		4		
	177.0	18	14			
	124.0				10	
	122.4	17	13			10
ACLP	105.0	16	12			
	102.0	15		3		
	99.0	14	11			
CORE TOP	94.0	13	10		6	
	93.1					7
CORE MID-PLANE	76.9					5
	76.0	9	6		4	
	75.1					4
CORE BOTTOM	58.9					2
	58.0	5	2		2	
	55.0	4	1			1
	54.0					1
	24.0	3				
NOZZLE PIVOT	15.0	2		2		
NOZZLE TIP	6.0	1		1		
	0					

Fig 3: Diagram of fuel assembly showing locations of load pads (Taken from *ASME/ANS bi-annual nuclear power conference report, Philadelphia, PA, 20 Jul 1986, pp. 446-453)*

The gas plenum exists between the ACLP and the TLP. Metallic fuel has poor fission gas retention and thus requires the additional space to hold fission gases without over-pressurizing the fuel and causing it to rupture.

Studies performed by ANL in 1986 used the structural analysis code NUBOW [9] to calculate the fuel bowing coefficients of the same reactor with two different core restraint systems.[10] The first core restraint method used the previously described restraint system that would later be employed by IFR. The second core restraint method utilized a ACLP and no TLP which allowed the fission plenum section of the fuel to "free flower" unrestrained. In the unrestrained, free-flower model, the maximum radial displacement occurs in the fission plenum section of the fuel assembly. The only part of the fuel assembly that can contribute negative reactivity is the active core region so ensuring that area receives

the most displacement was a prime objective. It was shown that by limiting the displacement of the gas plenum using the TLP, the active region of the assembly would displace the most, leading to the largest negative reactivity. Fig. 4 shows a graphic representation of these results. Each line represents a deformed fuel assembly, and it is easily seen that the "restrained", non-free-flowering assembly received the most displacement in the core region.
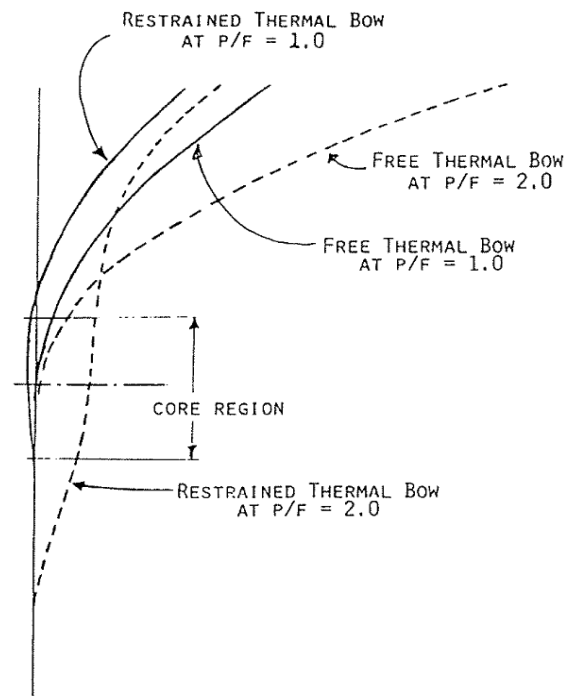

Fig. 4: Comparison of core restraint systems during transient (Taken from *ASME/ANS bi-annual nuclear power conference report, Philadelphia, PA, 20 Jul 1986, pp. 454-458)*

Chapter IV: Review of Existing Fuel Bowing Codes

Now that the history and importance of fuel bowing reactivity feedbacks have been established, it is important to examine what tools exist to calculate them.   There are two codes relevant to this discussion: ATLAS **[11]** and NUBOW **[9]**.   ATLAS is a code developed by Toshiba in 1995 that combines four smaller codes that calculate neutron flux distributions, temperature profiles, assembly deformations, and reactivity worths of the fuel assemblies. **[11]** The results of each of the sub-codes in ATLAS have not been extensively verified, and ATLAS is currently not available for commercial use. NUBOW was developed by Argonne National Lab and only requires as inputs the temperature profiles, neutron flux distributions, and reactivity displacement worths of each assembly in the core. **[9]** NUBOW is currently being overhauled and upgraded and is not currently available for commercial use. Thus, there are no currently available methods for calculating reactivity contributions due to fuel bowing. In order to generate fuel bowing reactivity coefficients for SABR, a calculation model will first be developed. This model will be described in detail, but it is worth first describing SABR, the reactor for which the model was designed.

Chapter V: SABR Overview

SABR is a fission-fusion hybrid reactor, an amalgam of the International Thermonuclear Experimental Reactor (ITER) and the IFR. **[1,12,2]** Its purpose is to close the back end of the nuclear fuel cycle by fissioning the transuranics (TRU) discharged from conventional LWRs. A cross section of SABR is shown below in Fig. 5.
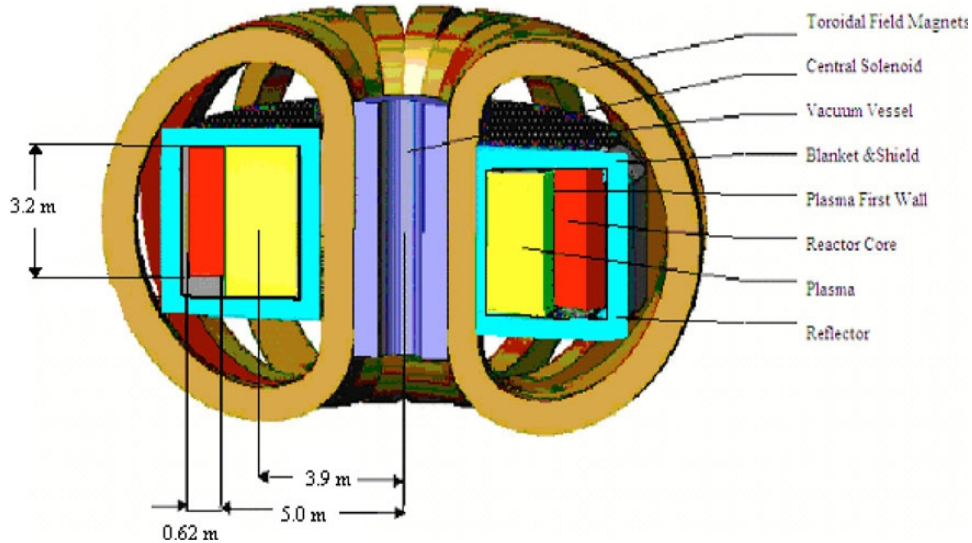

Fig. 5: SABR Cross-Section

SABR's 62cm thick annular fission core is a metal fueled, sodium cooled, pool type, 3000 MWt fast reactor, and its design is based heavily on IFR.**[1]** The fuel is 3.2m tall with an active length of 2m. The fuel is a TRU-Zr alloy developed and tested by ANL **[13]** and the clad is an ODS steel. There are 271 pins per assembly and a total of 918 assemblies divided up into 4 concentric rings as shown in Fig 6. The fusion neutron source is based on the same technology and plasma physics that is the basis of the ITER design and which will be demonstrated by ITER operation in the 2020s.

SABR is designed to produce 3000 MWth recoverable power, including the fusion power and power from exoergic reactions as well as the fission power. This power is used to produce electricity

using a conventional sodium-based secondary cycle. A table of SABR's thermal hydraulic parameters is shown in Table I. Fuel bowing is expected to be prevalent in SABR due to the strongly varying radial power profiles shown in Fig 7. The axial profiles are shown in Fig. 8. This power profile generates temperature changes across the rings that will be the main driver of fuel bowing in a transient. The steady-state axial distributions of sodium temperature and radial temperature difference for each ring are shown in Fig. 9 and Fig. 10.
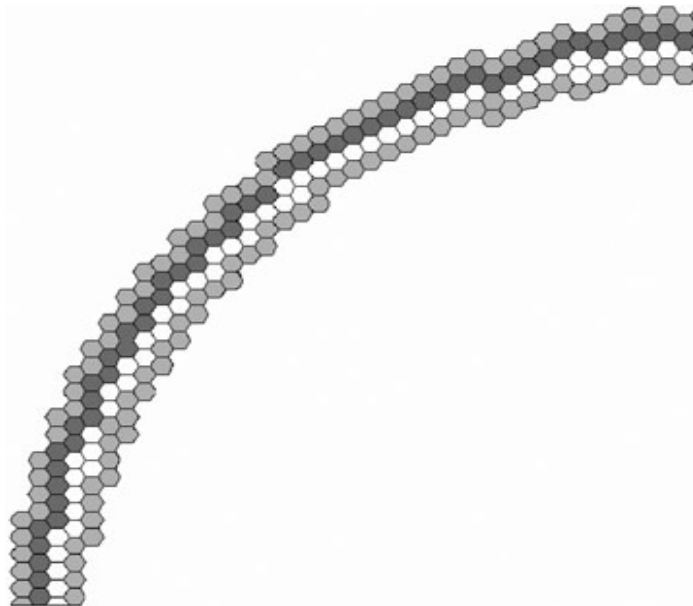

Fig. 6: Quarter Slice of SABR's Fission Annulus

Table 1: SABR Thermal Parameters

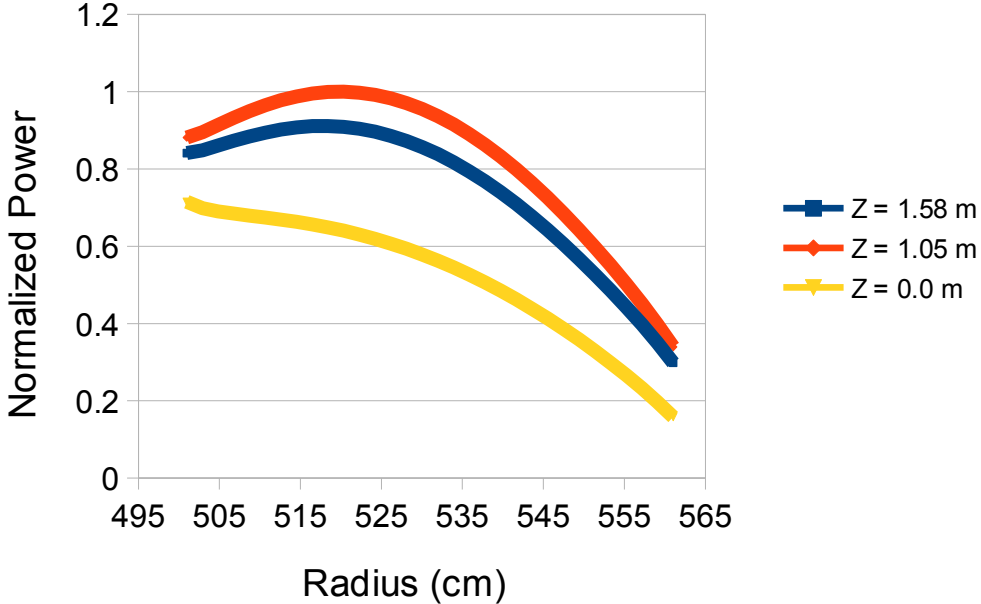|	
Power	3,000 MWt
Power Density	72.5 MW / m^3
Core Mass Flow Rate	16,085 kg/s
Core Inlet Temperature	698 K
Core Outlet Temperature	842 K
Secondary Mass Flow Rate	11,560 kg/s
Secondary Inlet Temperature	610 K
Secondary Outlet Temperature	810 K

Fig. 7: Radial Power Profile of SABR's Fission Core
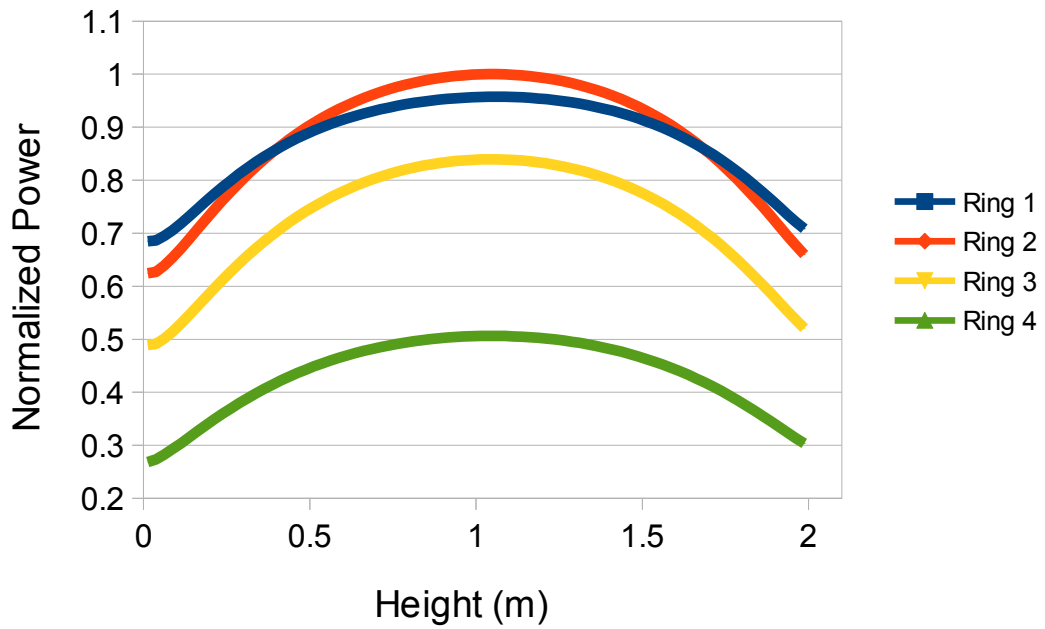
Axial Power Profiles

Fig. 8: Axial Power Profiles of SABR's Fission Core

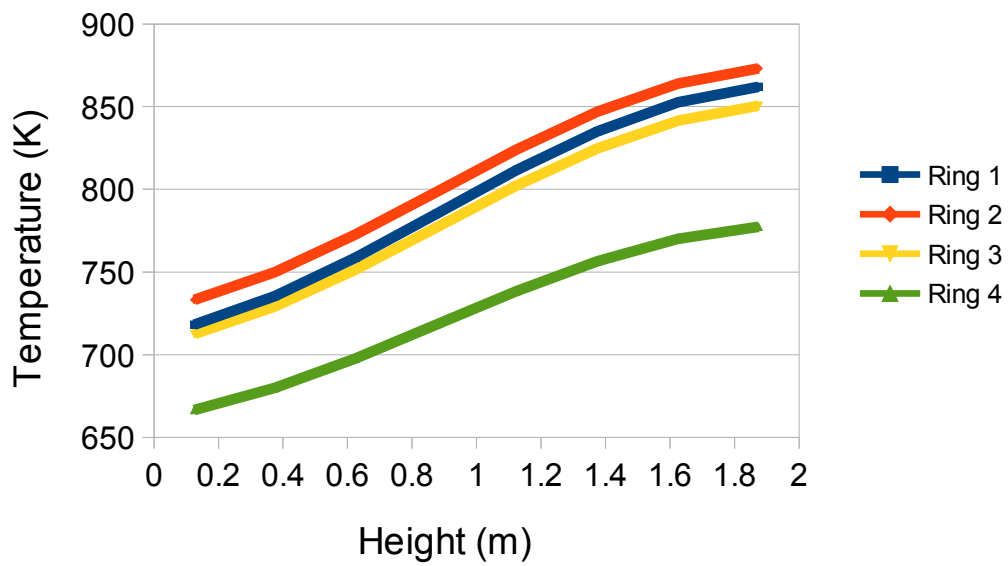## Axial Temperature Distribution of Sodium

Fig. 9: Axial Temperature Distribution of Sodium for Each Ring

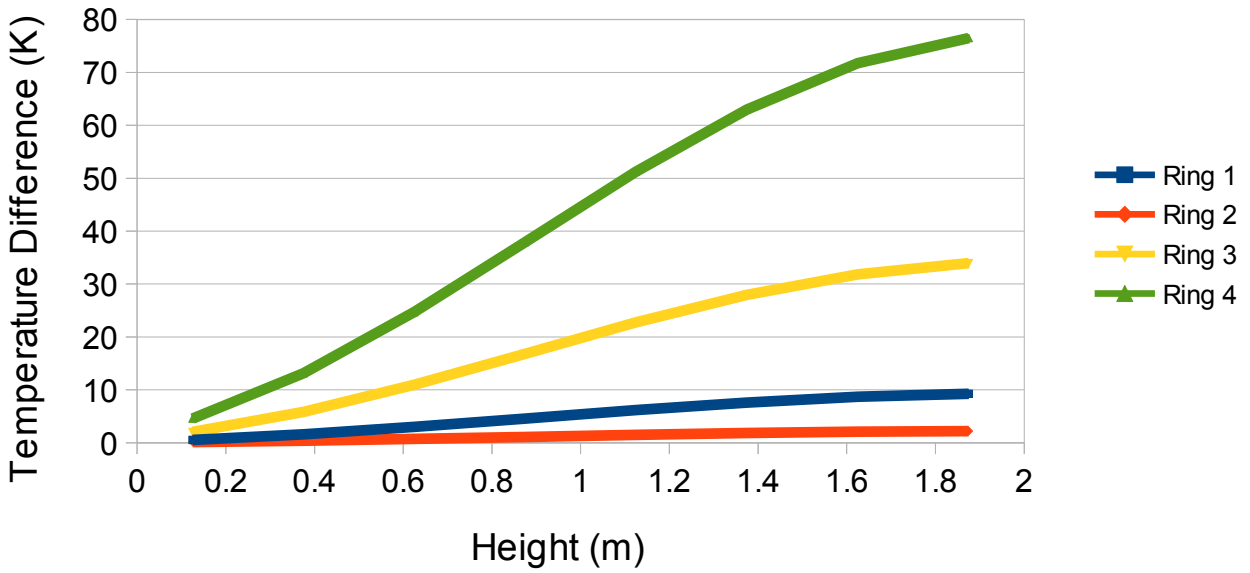# Axial Distribution of Radial Temperature Differences

Fig 10: Axial Distribution of Radial Temperature Differences Across Each Ring

Chapter VI: Fuel Bowing Reactivity Calculation Model

Passive safety is a very attractive feature of the IFR design, and it is critical to know whether or not SABR will exhibit similar behavior. The objective is to run a simulation of SABR's transient behavior (a Loss-of-Flow-Accident for example) and determine if the fuel bowing reactivity is sufficient to provide a net negative feedback under all transient conditions. To that end, a method for calculating the fuel bowing reactivity feedbacks has been developed. The method that has been developed has three distinct steps: 1) Calculate the temperature difference that develops across the fuel assemblies during a transient. 2) Find the deformed shape the assemblies will take based on these temperatures differences. 3) Calculate the reactivity change caused by the deformation of the fuel.

Temperature Gradients

The temperature gradients across the fuel assembly are calculated using RELAP5-3D. **[14]** RELAP5-3D is a thermal hydraulics code used to predict the transient behavior of nuclear reactors. The code also has a point kinetics model that is coupled to the heat removal calculations. This enables the user to integrate various nuclear effects such as feedback coefficients and control rod insertions into the analysis. This feature is used when calculating temperature gradients, but the only feedbacks considered when calculating these temperature gradients are doppler broadening and sodium voiding. These were the only two reactivity feedbacks considered when performing previous safety analyses for SABR.**[15]**

SABR's core is an annulus of four concentric rings of fuel assemblies as shown earlier in Fig 6. Because the fusion neutron source lies in the center of this annulus, the radial power distribution all of the fuel assemblies in a single ring will have the same radial power profile and therefore exhibit the same bowing behavior. This means that a fuel bowing analysis can be performed on a single characteristic fuel assembly from each ring instead of the entire core. To further simplify things a

subchannel analysis is performed on a single strip of each of these characteristic fuel assemblies as shown in Fig. 11. The power profile varies radially from row A to row S with row A being closest to the plasma; the radially outward direction moves from row A to row S.
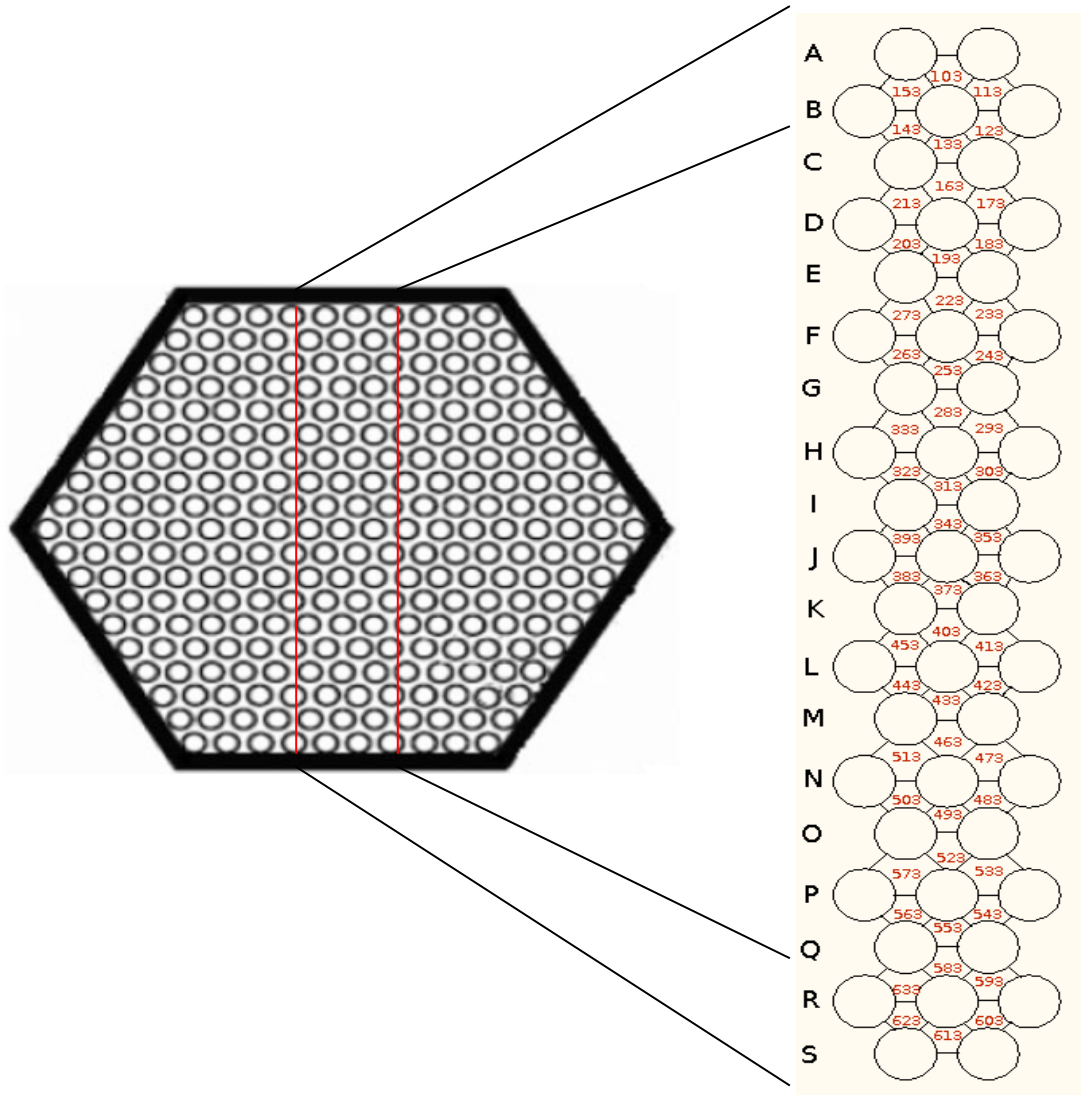

Fig. 11: Expanded view of RELAP subchannel model

RELAP is used to perform a subchannel analysis on the strip of a characteristic fuel assembly from each of the four rings. Each subchannel is assigned its own unique flow channel in RELAP. RELAP requires information on flow areas, axial and radial power distributions, and initial mass flow

rates for each of those unique flow channels. Cross-flow between subchannels is enabled in RELAP by creating a list of flow channels with which each individual channel can exchange fluid and energy. This is accomplished by using "multiple-junctions" in RELAP. An example of this would be listing that channel 103 (as shown in Fig. 11) can exchange energy and fluid with only channels 153 and 113. This process is repeated for every subchannel. A full representation of the RELAP model is shown in Fig. 12. The full primary loop and the Intermediate Heat Exchanger (IHX) are modeled, and the secondary loop is modeled as a boundary condition using two "time-dependent volumes" (shown in green). The loop splits into 54 subchannels (shown in red) each with a lower plenum, active fuel region, and upper plenum; only 2 of the 54 subchannels are shown in the figure for the sake of simplicity. The model requires a total of 62 "multiple-junctions" to properly couple the subchannels together.
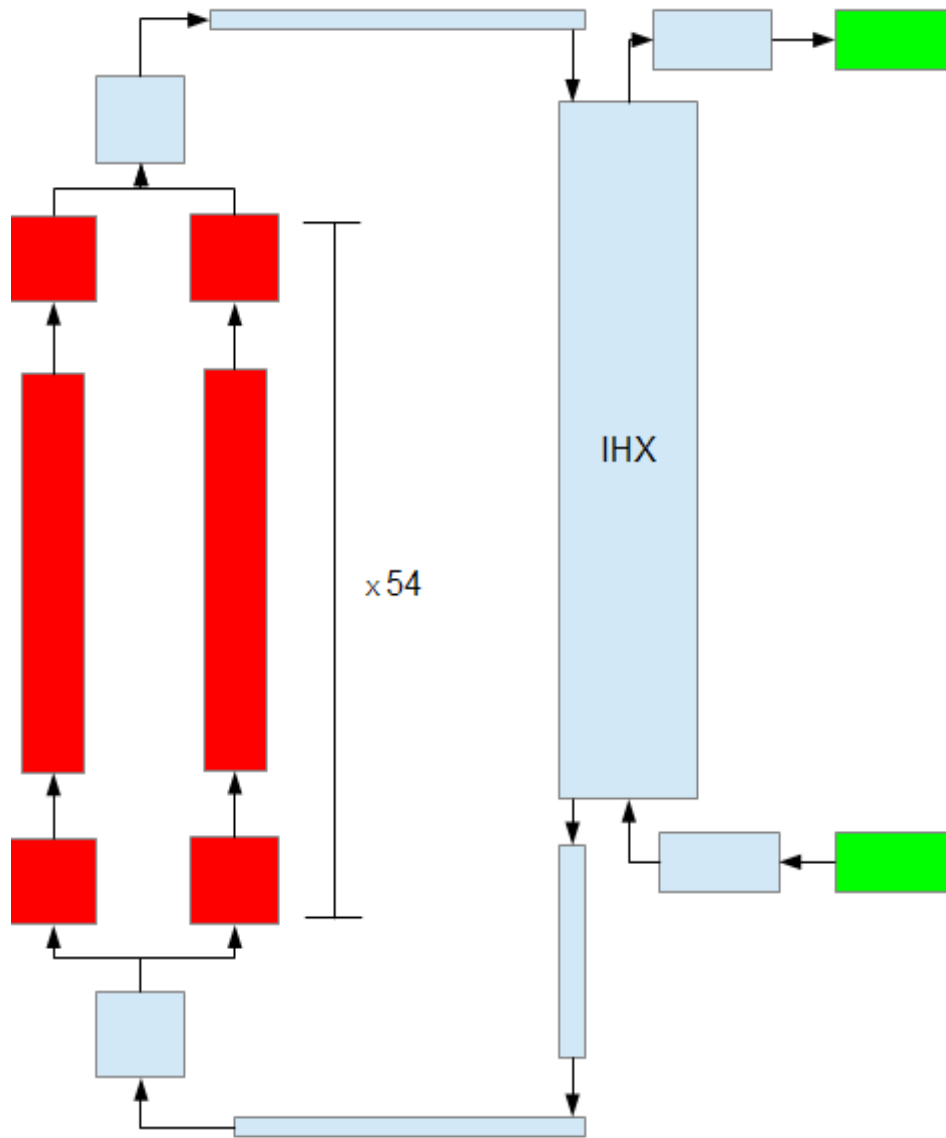
Fig. 12: Diagram of RELAP model

While RELAP-3D is primarily used to perform dynamic safety analyses of an entire reactor core, it can can also be used to perform a subchannel analysis. It is onerous work to set up the model and the calculation is computationally expensive, but it has been validated through the use of historical data. The result of these subchannel calculations is a large array of data that contains the sodium, clad, and fuel temperatures at eight axial points for every subchannel for numerous time steps. The temperature difference across the assembly (the main driver of fuel bowing) can be inferred by looking

at the sodium temperatures for channels 103 and 613. The channels lie at either end of the assembly, and it is assumed that the assembly wall will be at the same temperature as the sodium adjacent to it.

Fuel Assembly Thermal Displacements

Abaqus [16] is used to calculate the displacement of the fuel assembly structure, or duct, based on the temperature gradients from RELAP. Abaqus is a commercial finite element analysis code that can be used to solve a myriad of structural engineering problems. The Abaqus model for SABR is similar to the one in RELAP in that a single characteristic fuel assembly from each ring is included as shown in Fig. 12. In this case, the model only includes the duct portion of the assembly, i.e., the outer hexagonal shell. It is not necessary to include the fuel pins in a structural analysis because they do not place any significant load on the duct. It is assumed that the fuel pins will deform uniformly with the duct, ie the fuel pins will maintain their positions relative to one another as they deform.[4] Also visible in Fig. 12 is a small, immovable plate that represents SABR's core restraint ring. This restraint ring is loosely based on IFR's design [2]. Studies performed by ANL on EBR-II revealed that wrapping the core with a combination of restraint rings at various elevations helped the fuel bow out and away from the core during a LOFA quicker than if the fuel had not been restrained at all. [10] For simplicity, only one restraint ring has been put into the model. The temperature profiles from the RELAP calculations are input to the Abaqus model through the use of a customizable, user-written fortran subroutine.

The actual displacement calculation is made using finite element analysis (FEA). The mesh used to discretize the problem can be seen in Fig. 13. The FEA model used in this calculation is quite complex, involving the use of shell elements, thermal strain, and contact forces. The basic modeling can be illustrated by the case of a simple solid beam with a load applied to one end. A system of equations of the form shown in Eq. 1 is generated. F is a vector containing the forces applied to the element at various points, k is a matrix of stiffness coefficients that are a function of material properties

20

and geometry, and u is a vector containing the resultant displacements and bending moments. The resulting system of equations is then solved numerically (usually iteratively).

$$F = \mathbf{k}\, u \qquad (1)$$
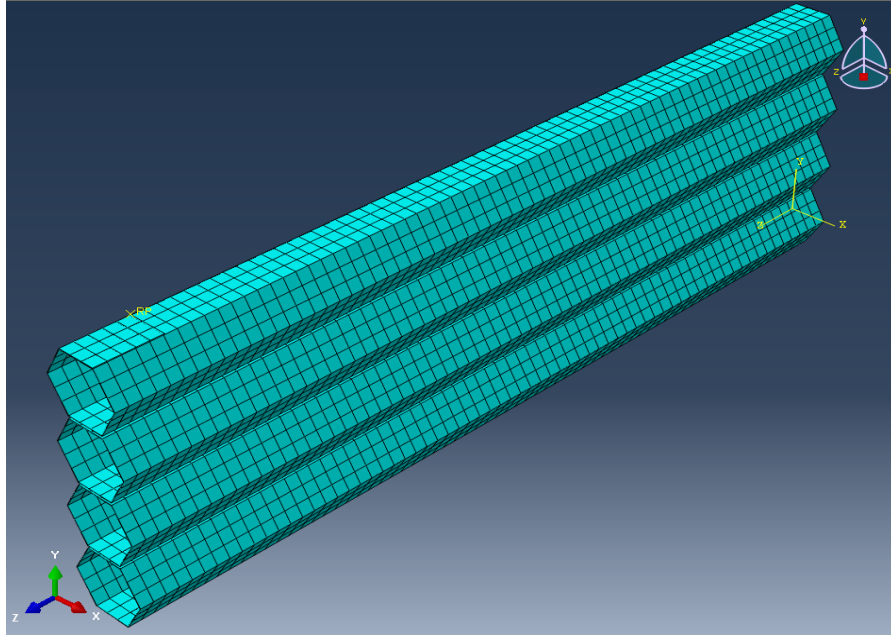
Fig. 13: The Abaqus model of SABR

The end result of these calculations is a file containing the displacements in the x, y, and z directions at every mesh point. Generally, the displacements in the radial direction are several orders in magnitude greater than the others, so the displacements in the non-radial directions are ignored and the deformed duct is mapped into eight undeformed axial slices that have simply been displaced in the radial direction (y-axis in Fig. 13) as shown in Fig. 14. This is done to enable a simpler computation of the change in reactivity due to the fuel deformation.

Fig. 14: Mapping of the bowed shape into axial slices

Neutron Transport Model

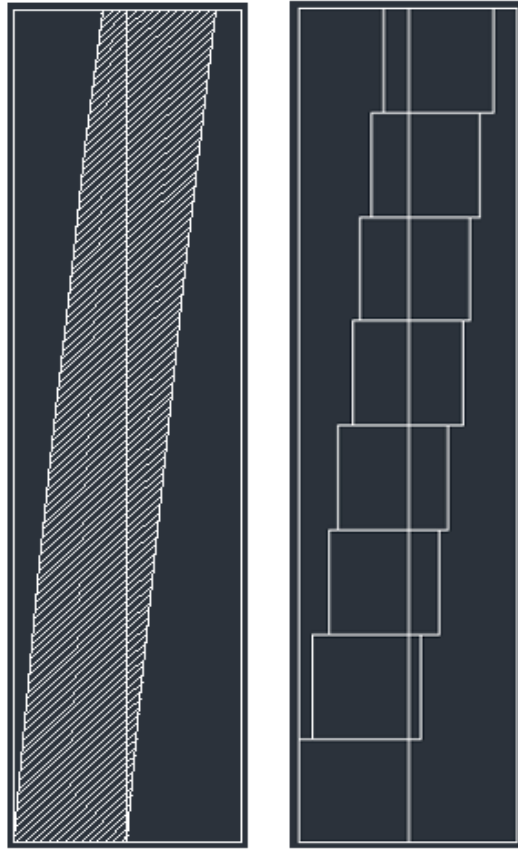The reactivity worths of the fuel displacements are calculated using ERANOS[17]. ERANOS is a multifaceted fast reactor neutronics code that contains deterministic diffusion and transport solvers, perturbation modules, and a fine group cross-section library. ERANOS can calculate transport solutions for multiplying systems driven by an external neutron source and can make perturbation calculations as well. The SABR neutronics model was adapted from a previous model used for fuel cycle calculations.[18] The model is an RZ slice of SABR and can be seen in Fig. 15. Each of the four rectangles in the "fission core" represents one of the four rings in the fission annulus. There are 216 axial mesh points and 185 radial mesh points. The ERANOS module ECCO calculates the cross-sections using the JEFF 2.0 library with a 33-group structure. The module BISTRO performs the transport calculations using discrete ordinates with an S8 quadrature using the "DIAMANT_TETA"

22

option for the difference scheme. A diffusion-accelerator is utilized to reduce the required number of iterations. The numerical convergence is set to 1e-5 for the multiplication factor.
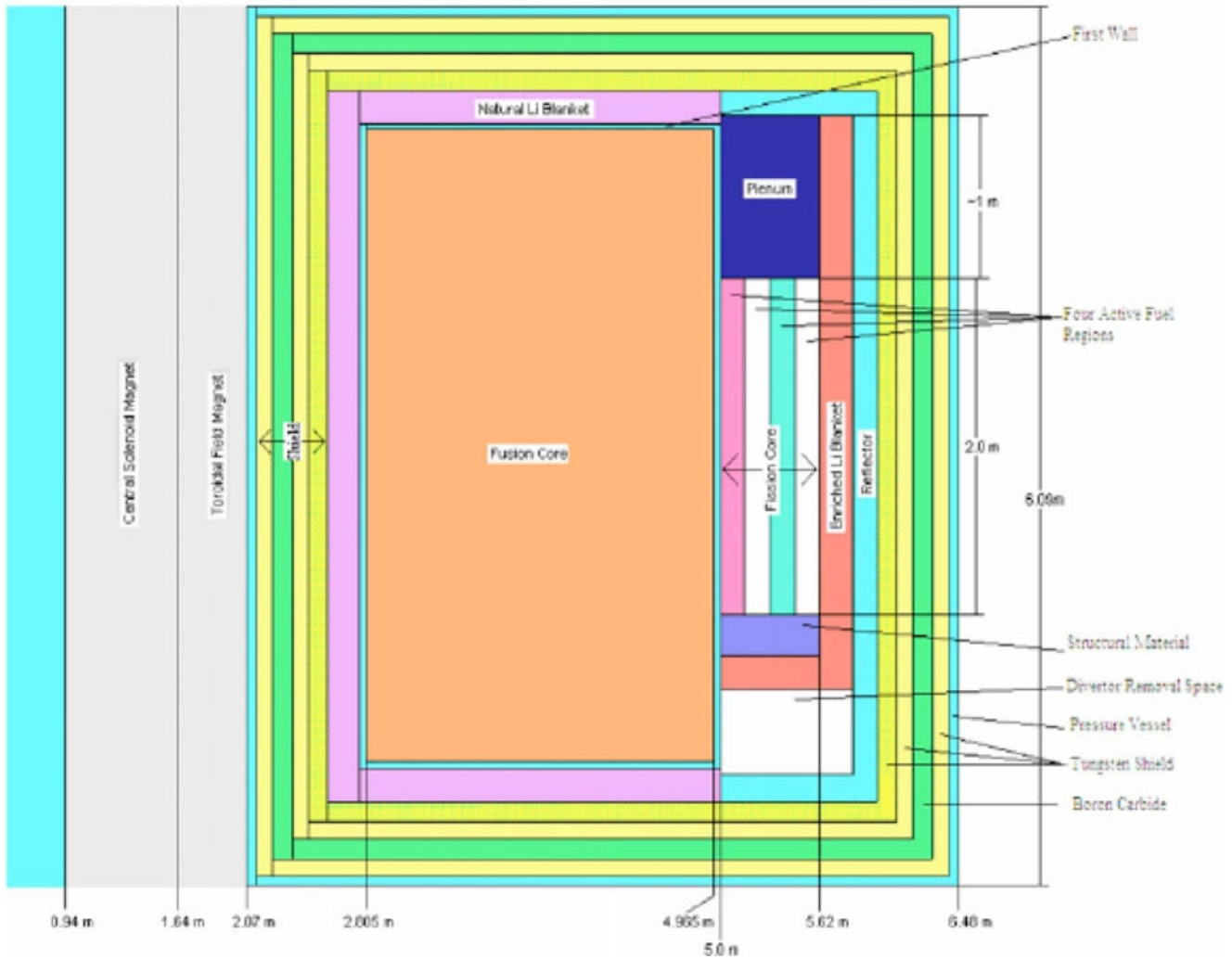
Fig. 15: Cross-Section View of SABR's RZ model in ERANOS

Reactivity of Fuel Displacement

ERANOS calculates the associated change in reactivity through the use of transport-based, first-order perturbation theory[19] as shown in Eq. 2. The δk term is the change in reactivity, k_o is the k-effective value of the unperturbed state, ψ^a is the sourceless (λ-mode) adjoint flux solution generated by ERANOS, ψ is the sourceless (λ-mode) direct flux solution (also generated by ERANOS), G is the

23

fission operator, and H is the transport operator.

$$\frac{\delta k}{k_o^2} = \frac{[\psi^a(k_o^{-1}\delta G - \delta H)\psi]}{[\psi^a G \psi]}$$

(2)

Both operators are functions of the cross-sections sets, and ERANOS calculates the changes in these operators based on the perturbed cross-section sets entered by the user. Strictly speaking, the calculation of an adjoint flux solution for a system with an external source should be made, which requires the definition of a separate "adjoint source". For the purposes of calculating a change in k-eff, the adjoint source is mathematically equivalent to the fission cross-section of the fuel. Since studies have shown that using the critical (λ-mode) sourceless flux and adjoint solutions in first-order perturbation calculations for source problems works quite well, we adopt this option.[20] It is also worth noting that k is defined differently in a sub-critical, source-driven system than it is for a sourceless critical system. For the critical system, k becomes the familiar k-effective which is the number of fission neutrons consequently produced by a single incident fission neutron. For the source-driven system, k takes the form of k-source which is the number of fission neutrons generated per source neutron emitted. In order to input the perturbations the user can either supply the perturbed and reference macroscopic cross-section sets or supply a single microscopic cross-section set with two concentrations sets for the reference and perturbed cases. The former method is utilized in this work. The user generates the perturbed cross-section sets by adjusting the densities of various materials in the ERANOS model. For example, the user could change the density of all of the sodium in the core to simulate voiding. The ERANOS cross-section processor ECCO is used to generate a cross-section set for the voided core. Then the perturbation module in ERANOS is run using the perturbed and reference cross-section sets along with the direct and adjoint flux solutions. This is normally a simple process but not when performing a perturbation calculation for fuel bowing. This is because the perturbation comes in the form of geometry changes instead of overall cross-section changes. The key

24

to making the calculation is mapping a geometric perturbation into macroscopic cross-section perturbations in a fixed geometry. This is best accomplished in ERANOS by breaking the fuel assemblies up into many sub-regions or "bow zones" as shown in Fig 16.
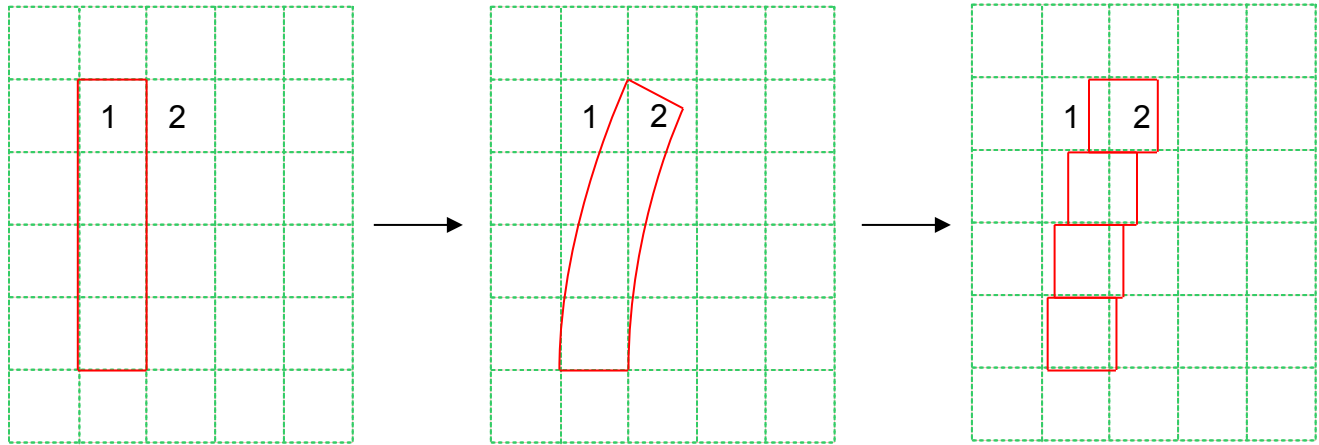
Fig. 16: Fuel bow zone mapping

The figure above is far simpler than the actual one used for SABR, but it illustrates the same concept of converting a change in geometry to a change in macroscopic cross-sections in a fixed geometry. Each one of the green squares represents a different homogenous material and cross-section set in ERANOS. The red rectangle represents a homogenized fuel assembly that undergoes bowing. To convert this deformation to a change in macroscopic cross section, the user first maps the deformed shape in the second part of the figure to the approximated slices shown in the third part of the figure. Next, the new volume fractions are calculated for each of the materials as shown in Table II.

Table 2: Example Fuel Bowing Volume Fractions

	Unbowed (Reference Case)		Bowed (Perturbed Case)	
	Material 1	Material 2	Material 1	Material 2
Fuel Vol Fraction	1.00	0.00	0.33	0.67
Moderator Vol Fraction	0.00	1.00	0.67	0.33

ECCO uses these new volume fractions to generate another cross-section set for the "perturbed" case. A MATLAB program has been written that takes in the one-dimensional displacements calculated by ABAQUS discussed earlier and calculates the new volume fractions that are input to the many different bow zones in ERANOS. Once the perturbation calculation is complete, ERANOS outputs the results in the form of a single number, call it V, that is defined by Eq. 3. Using this equation the new reactivity can be calculated.

$$V = \frac{(k' - k)}{(kk')}$$

(3)

Where V = Number generated by ERANOS perturbation calculation, k = Reference case k-eff, and k' = Perturbed case k-eff

Chapter VII: Verification of Fuel Bowing Reactivity Model

Calculations using the models described in the previous section have been made on simple configurations that can be calculated by hand in order to ensure that the codes are indeed solving the equations as intended.

RELAP Subchannel Model Verification

This subchannel model was validated by temporarily disabling cross-flow and then performing an energy balance on a single subchannel by solving for the outlet temperature of the sodium using Eq. (4).

$$T_o = \frac{\dot{Q}}{(\dot{m}) c_p} + T_i$$

$$\text{(4)}$$

where T_i = Inlet temperature taken from RELAP (K), T_o = Outlet temperature (K) ,m_{dot} = Mass flow rate taken from RELAP (kg/s), c_p = Average specific heat capacity (kJ/kg*K) and Q_{dot} = Total channel heat rate taken from RELAP (kW).

The heat rates, mass flow rates, and inlet temperatures used in the hand-calculation were taken from RELAP and used to calculate the outlet temperature. The heat capacity data of sodium was taken from the literature.[21] This calculation was performed for two different subchannels, channels labeled 103 and 613 in Fig. 11. These channels lie at opposite ends of the fuel assembly and are used to calculate the temperature difference across the assembly. The results from the hand calculation and the RELAP model agree very well as shown in Table III. The temperature gradients between channels 103 and 613 as calculated by the RELAP temperatures and the hand-calculated temperatures agree to within 0.5%.

Table 3: Data Used in RELAP Verification

	Hand		RELAP	
	Channel 103	Channel 613	Channel 103	Channel 613
m_{dot} (kg/s)	5.53E-002	5.56E-002	N/A	N/A
Q_{dot} (kW)	11.97	4.4	N/A	N/A
c_p (kJ/kg*K)	1.27140	1.25918	N/A	N/A
T_i	741.66	741.66	741.66	741.66
T_o	913.84	804.54	914.04	804.63

Fuel Assembly Deformation Model Verification

The Abaqus model was also validated via hand-calculations.[22] A solid 6cm x 6cm rectangular stainless steel block 1m in length was created in ABAQUS and put under a uniform 100 K temperature change. The resulting displacement was compared to the one that was hand-calculated by Eqs. (5.1), (5.2), and (5.3). Eq. 5.1 is a basic application of the thermal strain equation in rectangular geometry, Eq. 5.2 is the resulting bending moment induced by the temperature difference, and Eq. 5.3 is the 2nd moment of inertia for a rectangular geometry. The simple geometry of a solid rectangular block was chosen because it was the easiest geometry in which to make a hand-calculation of the displacement. The ABAQUS model calculated the maximum displacement to be 1.48 cm while the hand-calculated maximum displacement was 1.46 cm, a less than 1.5% difference.

$$U_{Tx} = \frac{M_{Ty} L^2}{2EI_{yy}}$$
(5.1)

$$M_{Ty} = \iint \alpha E T_x x^2 \, dy \, dx$$
(5.2)

$$I_{yy} = \frac{hw^3}{12}$$
(5.3)

Where U_{Tx} = Thermal strain in the x-direction (m), M_{ty} = Bending moment (N*m), L = Length of block in the z-direction (m), E = Young's Modulus of Elasticity (Pa), I_{yy} = Second moment of area (m⁴), α = Thermal expansion coefficient (m/K*m), T_x = Temperature gradient in the x-direction (K/m), h = Height of the block in the y-direction (m), and w = Height of the block in the x-direction (m).

Reactivity Model Verification

The ERANOS model was not verified with hand-calculations; instead a direct calculation of reactivity for the perturbed case was made and compared to the perturbation theory estimate. This was done because the accuracy of a perturbation calculation is dependent on the size of the perturbation. If the model was verified with a small perturbation, and then later that same model is used with a larger perturbation, the benefit of verification would be lost. Thus, when any series of fuel bowing calculations is made using the ERANOS model, the specific calculation with the largest change in reactivity should be checked against a direct calculation of reactivity. The procedure is performed in the following section where some sample fuel bowing calculations are presented.

Example Fuel Bowing Calculation

Now that the procedure for calculating fuel bowing coefficients has been presented, it is useful to show an actual example calculation. The scenario chosen for this example is a 50% Loss-of-Flow-Accident for SABR. The calculations were performed for several time steps during the transient: t = 0s (steady state), t = 3.3s, t = 5.3s, t = 7.1s, t = 9.7s, t = 13.8s, and t = 67.8s. A time step was assigned every time the largest temperature difference in the core rose by 50K until an asymptotic behavior was reached. The coast down of the core mass flow rate is shown in Fig. 17, and the resulting temperature differences at the top of each of the assemblies are shown in Fig. 18. Table IV shows the displacements and reference elevations for the axial slices in each of the characteristic assemblies during the t = 7.1s time step. Positive displacements signify radially outward movement while negative displacements

29

signify radially inward movement.

Finally, the associated change in reactivity is shown in Fig. 19. It is worth noting that the reactivity increases toward the end due to the over-simplified core restraint system described earlier. Including the multiple restraint rings and the fission gas plenum in the ABAQUS analysis would prevent the slight increase in reactivity due to fuel bowing shown in these results. [10] The reactivity calculation was verified by performing a direct reactivity calculation of the perturbed system from the t = 7.1s time step as that one had the largest change in reactivity. The perturbation estimate of the variation was V = -3.2e-3 while the direct calculation of the variation was -3.14e-3. The results agree to within 2% for the largest perturbation calculation, so the reactivity calculations can be considered accurate.
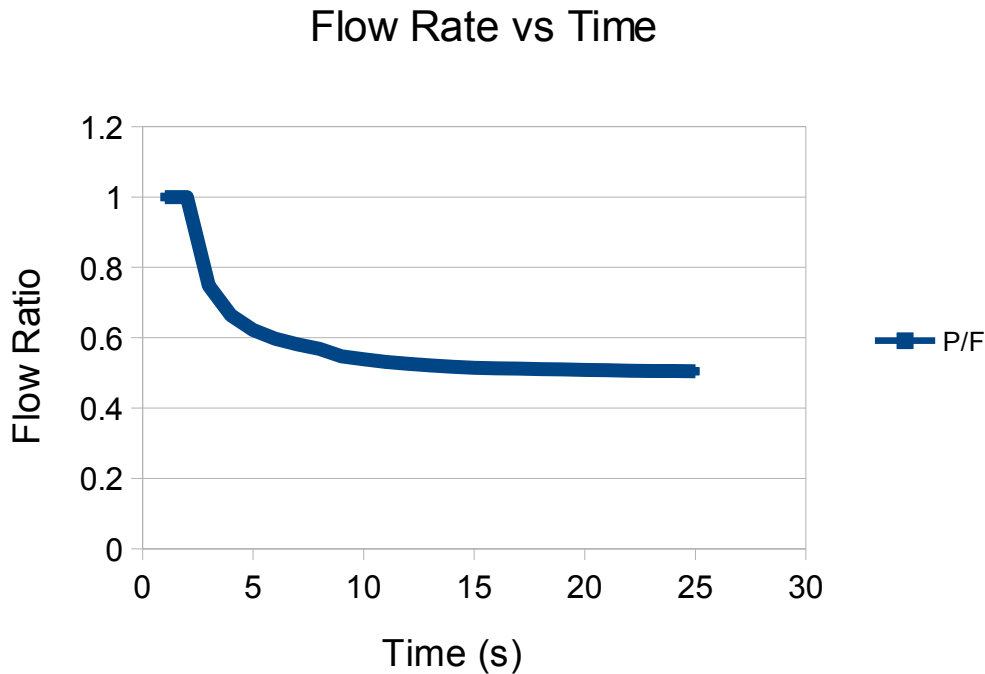
Flow Rate vs Time

Fig. 17: Core Flow Mass Flow Rate Coastdown

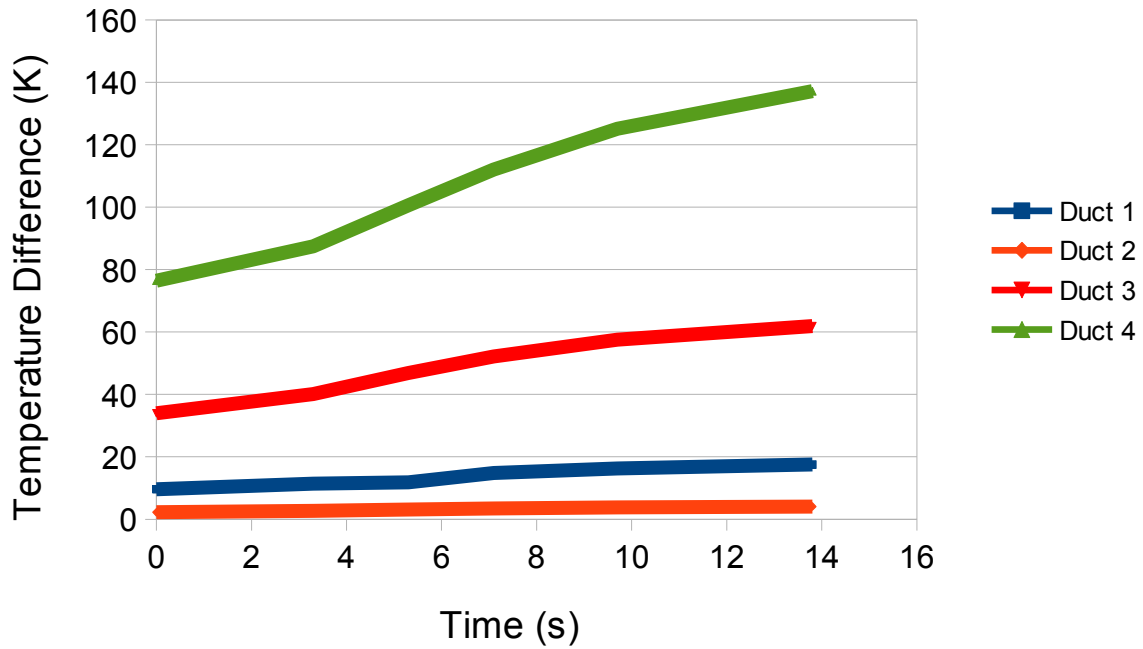# Radial Temperature Differences at Top of Fuel Assembly

Fig. 18: Radial Temperature Differences for 50% LOFA

Table 4: Fuel Assembly Displacements for 50% LOFA

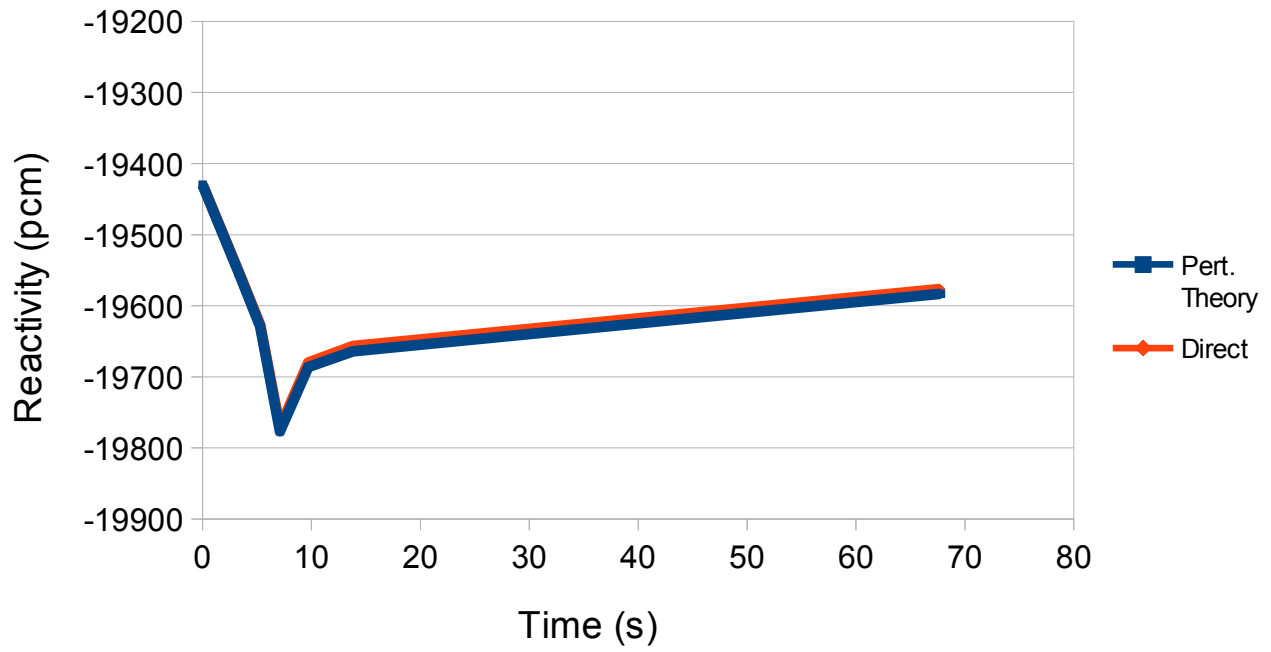| Height of Axial Slice	Assembly 1	Assembly 2	Assembly 3	Assembly 4
1.875 m	-1.68 mm	0.44 mm	6.56 mm	2.26 mm
1.625 m	-1.33 mm	0.35 mm	5.22 mm	1.75 mm
1.375 m	-0.99 mm	0.26 mm	3.93 mm	1.37 mm
1.125 m	-0.74 mm	0.19 mm	2.91 mm	1.15 mm
0.875 m	-0.47 mm	0.12 mm	1.84 mm	0.8 mm
0.625 m	-0.24 mm	0.06 mm	0.94 mm	0.26 mm
0.375 m	-0.08 mm	0.02 mm	0.33 mm	-5.87 μm
0.125 m	-0.74 μm	3.73 μm	26.6 μm	-78.6 μm

Fig. 19: Fuel Bowing Reactivity Change for 50% LOFA

Chapter VIII: Conclusions

A model has been developed for calculating the change in reactivity due to the thermally-driven movement of fuel assemblies during a transient such as a Loss-of-Flow-Accident. All three components of this calculation: temperature, fuel motion, and reactivity, have been shown to be accurate, and the calculational model is easily adaptable to model other fast reactors.

There are several drawbacks to this method however, all of which are related to efficiency. RELAP was not designed to perform subchannel analyses. Although it has been shown to do so accurately, it does not do so efficiently.[23] The difficulty arises not in the computation time, but in the time it takes to generate the input file. Each individual subchannel requires a large amount of code to model, and the internal numbering and identification system that RELAP employs puts a limit on the total number of channels that can be modeled at once. Also, generating the subroutine that defines all of the temperatures for the ABAQUS model requires a large amount of tedious cut-and-paste work with the RELAP output file. Additionally, it takes a bit of work converting the displacements given by ABAQUS into a new medium concentration for a section of fuel, but that was facilitated by the creation of a MATALB script. ABAQUS requires the Intel Fortran Compiler to compile the subroutine when the problem is run. The Intel Fortran Compiler is one of the most expensive fortran compilers available, and no other fortran compiler can be used with ABAQUS nor can the subroutine be compiled separately from ABAQUS. Fortunately, ABAQUS computation time or convergence is not an issue with this model.

While the ABAQUS and RELAP models have minor efficiency problems that can be negated by writing various "helper" codes to quicken data transfer between programs, ERANOS is a little more stubborn. The idea behind the use of perturbation theory is that a change in reactivity can quickly be calculated given a change in cross-section. This is somewhat lost in the ERANOS model because even

though the actual perturbation calculation takes only a few seconds, the cross-section processing it requires takes several hours. The reference set of cross-sections is stored in an archive file, but a new cross-section set must be generated for each time step of the transient. The perturbation module of ERANOS was designed so that a user would not have to do this; it allows the user to select a medium or nuclide and then multiply its initial concentration by a single coefficient. No matter how many nuclides or media are being perturbed, ERANOS only accepts one coefficient, so everything gets perturbed by the same amount. This will not work in a fuel bowing calculation because every medium is perturbed by a different amount. It would also be far too inefficient to perturb one medium at a time and use super-position to calculate the full change in reactivity.

One potential solution to this problem that will explored in the future is generation of a table of sensitivity coefficients for SABR. This is accomplished using variational perturbation theory (VPT). Variational perturbation theory differs from first-order perturbation theory in that it accounts for the change in flux as well as the change in macroscopic cross section caused by the perturbation. This is done not by calculating the perturbed flux but applying a "flux correction factor".[24] It remains to be determined what codes are capable of making these calculations.

References

1. W. M. STACEY, et al., "A TRU-Zr Metal Fuel, Sodium Cooled, Fast Subcritical Advanced Burner Reactor", *Nucl. Technol.* **162**, 53 (2008).

2. C. TILL, Y. CHANG, *Plentiful Energy: The Story of the Integral Fast Reactor*, p. 42, CreateSpace (2011).

3. H. HUMMEL, D. OKRENT, *Reactivity Coefficients in Large Fast Power Reactors*, pp. 82-183, American Nuclear Society (1970).

4. T. THOMSON, J. BECKERLEY, *The Technology of Nuclear Reactor Safety, Volume 1: Reactor Physics and Control,* pp. 530-607, Massachusetts Institute of Technology, Cambridge, Massachusetts (1964).

5. W. STACEY, *Nuclear Reactor Physics*, p.165, John Wiley & Sons, Inc (2001).

6. "Argonne History.", http://www.anl.gov/photos/argonne-history-1950s.

7. H. PLANCHON, et al, "Results and Implications of the Experimental Breeder Reactor II Inherent Safety Demonstration Tests," *Nuclear Science and Engineering,* **100**, 549-557 (1988).

8. D. WADE, R. HILL, "The Design Rationale of the IFR," *Progress in Nuclear Energy*, **31**, 13-42 (1997).

9. S. KAMAL, Y. ORECHWA, "Bowing of Core Assemblies in Advanced Liquid Metal Fast Reactors," *Joint ANS/ASME Nuclear Power Conference,* 1986.

10. T. J. MORAN, "Core Restraint Contributions to Radial Expansion Reactivity", *Joint ANS/ASME Nuclear Power Conference,* 1986.

11. M. NAKAGAWA, et al, "Development of the core-bowing reactivity analysis code system ATLAS and its application to a large FBR core," *Nuclear Engineering and Design,* **157,** 15-26 (1995).

12. "International Thermonuclear Experimental Reactor", http://www.iter.org/ (2013).

13. S. HAYES and M. MEYER, Argonne National Laboratory, Personal Communication (2007).

14. "RELAP 5-3D", http://www.inl.gov/relap5/.

15. T.S. SUMNER, et al., "Dynamic Saffety Analysis if the SABR Subcritical Transmutation Reactor Concept", *Nucl. Technol.* **171,** 123 (2010).

16. "Abaqus Unified FEA", http://www.3ds.com/products/simulia/portfolio/abaqus/ (2013).

17. G. RIMPAULT, et al., "The ERANOS Code and Data-System for Fast Reactor Analyses," *Proc. Int. Conf. New Frontiers of Nuclear Technology: Reactor Physics, Safety and High-Performance Computing (PHYSOR 2002),* Seoul, Korea, October 7-10, 2002, American Nuclear Society.

18. C. M. SOMMER, et al., "Fuel Cycle Analysis of the SABR Subcritical Transmutation Reactor Concept", *Nucl. Technology.* **172**, 48 (2010).

19. E. LEWIS, W. MILLER, *Computational Methods of Neutron Transport*, p55, American Nuclear Society, Inc, La Grange Park, IL (1993).

20. Y. KIM, et al., "Reactivity Estimation for Source-Driven Systems Using First-Order Perturbation Theory," *Proc. Int. Conf. New Frontiers of Nuclear Technology: Reactor Physics, Safety and High-Performance Computing (PHYSOR 2002),* Seoul, Korea, October 7-10, 2002, American Nuclear Society.

21. Y. TANG, et al., "Thermal Analysis of Liquid Metal Fast Breeder Reactors", ANS, 1978.

22. B. BOLEY, *Theory of Thermal Stresses*, p. 310, John Wiley and Sons (1960).

23. M. MEMMOT, et al., "On the use of RELAP5-3D as a subchannel analysis code", *Nuclear Engineering and Design*, **240**, pp. 807-815 (2010).

24. W. STACEY, "An Improved Reactivity Table Model for Liquid Metal Fast Breeder Reactor Dynamics", *Nuclear Science and Engineering*, **49**, pp. 213-227 (1972).